

# Wicking Phenomenon in Nanofiber-Coated Filament Yarns

Seyed Abdolkarim Hosseini Ravandi, PhD, Razieh Hashemi Sanatgar, MD, Farzad Dabirian, PhD

Isfahan University of Technology, Isfahan, Isfahan IRAN

Correspondence to:

Seyed Abdolkarim Hosseini Ravandi email: [hoseinir@cc.iut.ac.ir](mailto:hoseinir@cc.iut.ac.ir)

## ABSTRACT

Wicking phenomenon has been investigated in filaments and spun yarns in different studies. In comparison with conventional structures, nanofibrous structures have unique characteristics such as higher surface-to-volume ratios, smaller pores, and higher porosity. For many nanofiber applications, a good understanding of the liquid absorption and wettability of nanofibrous is crucial.

In this article, a modified electrospinning process for yarn coating with nanofiber is presented. In this method, fiber direction was controlled by manipulating the conventional system of electrospinning and embedded nanofibers on yarn surface. Nylon66 filament was coated with nylon 66 nanofiber. The coating morphology and capillary phenomenon were examined in different concentrations of polymer solution. The kinetics of capillary flow of colored liquid in coated yarns with nanofiber follows the Lucas-Washburn equation.

Results show that coating with nanofibers increases equilibrium wicking height. In a nanofiber coating process, with a constant feeding rate, increasing the solution concentration increases the capillary rise rate.

**Keywords:** electrospinning, nanofiber, coating, capillary, nylon, filament.

## INTRODUCTION

The behavior of a textile during its contact with liquid is one of the important properties of textiles [1]. Inter-fiber space in fibrous materials, such as yarn is in the form of capillaries that can be occupied by liquid. Because of this, wetting and wicking are important phenomena in their processing and applications [2]. A spontaneous transport of a liquid driven into a porous system by capillary forces is termed wicking. Wicking is a result of spontaneous wetting in a capillary system [3]. Capillary

phenomena occur when the free energy of the solid-gas interface exceeds the free energy of the solid-liquid interface [4]. There are several techniques for capillary flow analysis, including spontaneous liquid wicking analysis for yarn structure. These methods measure the time required for a liquid to wick into a certain length of yarn [5]. Various parameters, such as yarn structure, yarn tension, twist, fiber shape, number of fibers, fiber configuration, finishing, and surfactants control capillary size and its continuity influence wicking of yarns [6, 7, 8].

Sengupta and Murthy [9] reported that the wicking time of open-end spun yarn, for any given vertical wicking height, is less than that of ring-spun yarn due to inter-fiber pore structure. Chattopadhyay and Chauhan [10] studied the wicking behavior of ring and compact spun yarns. The rate of water rise was very fast at the beginning and slowed down gradually. The equilibrium wicking heights for ring yarns were more than compact yarns and ring yarns were wicked faster than compact yarns. Sengupta *et al.* [11] investigated the wicking behavior of air-jet textured yarns. For the same percentage of floats and arcs, trilobal filament yarns show better wicking properties, and a higher percentage of floats and arcs tend to increase equilibrium wicking height. As a result, many parameters such as yarn geometry, spinning systems, fiber types can affect the wicking phenomenon.

Some researchers [12, 13] investigated the wicking behavior of yarns produced with varying twist levels. Twisted filament yarn shows a lower wicking rate than a yarn without twist. The change in the wicking time with twist is due to a reduction of capillary size. In capillary penetration of liquids, tortuosity affects wicking. Twists in the yarns influence the size of inter-fiber capillaries as a result of the helical path of the fibers in the yarn.

According to Hollies *et al.* [14], increasing yarn roughness due to random arrangement of its fibers gives rise to a decrease in the rate of water transport. This work focuses on capillary rise in a new product in fiber assemblies, using electrospinning process to produce coated yarns with nanofibers.

Many coating techniques such as drop coating, melt coating, chemical vapor deposition and dip coating have been extensively used to produce functional coatings on fibrous yarns [15-19]. These coatings can add certain properties such as mechanical stability, abrasion resistance, chemical resistance, smoothness, as well as color or design effects. Electrospinning offers a flexible technique capable of enabling coating of nanofibers onto textile fabrics and implant stents [15, 20, 21].

Nanostructured yarns have potential applications in electronic textiles [22], ballistic protection fabrics [23], and tissue engineering, including artificial muscles [24-27]. For example, in biomedical engineering applications, scaffold porosity is a critical feature, as it controls free migration of cells. The pore sizes required for different cells may vary and must be at least equal to the size of a cell, about 10  $\mu\text{m}$ . However, in many cases, pore sizes of several 100  $\mu\text{m}$  are also necessary for optimal cell migration. Nanofiber webs usually result in low porosities and small pore sizes that may limit the use of nanofibrous scaffolds. Recently published studies show that combining nano and micro fibers in a scaffold may result in a beneficial structure [27]. Nanofibers provide surfaces for cell attachment and proliferation, while the micro fibers provide structural strength [27]. The proposed setup described in this contribution may open a new avenue for creating a combined yarn exhibiting nano and micrometer features.

Electrospinning is a known process for forming fibers with nano-scale diameters through the action of electrostatic forces. Any electrospinning equipment consists of four main parts: metallic capillary, high voltage source, pump and a collector. In typical electrospinning process, an electrical potential is being applied to polymeric droplet flow out from the tip of the needle. Droplet charging results in the Taylor Cone formation. When the electrical forces (electrostatic and coulomb force) overcome the surface tension of polymer solution, a charged fluid jet is ejected, following a spiral path. The electrical forces elongate the jet thousands of times and the jet stretches toward the grounded electrode, collecting on it randomly [28, 29].

Nanoscale structures have larger specific surface-to-volume ratios, higher porosity, and smaller pore sizes in contrast to macroscale nonwovens. Because the roughness of nanofiber mats is determined on the nanolevel, they have a very flat surface [30]. Also, the mechanical performance is superior to that of other forms of the same material [31]. Because of the large specific surface area, these structures absorb fluids very efficiently [32]. Other important properties are malleability [33] and ease of fiber modification [34].

For many applications such as biomedical applications [35], protective clothing [36], composites [37], filtration [38] and electrical and optical applications [39], a good understanding of the liquid absorption and wettability of nanofibrous is crucial. Jabal *et al.* [40] investigated the hydrophilicity of poly(vinylpyrrolidone)-titania nanofibers with contact-angle measurements. As a result, it was found that fiber mats baked at 200  $^{\circ}\text{C}$  for 24 h have excellent mechanical properties with wetting being even against frequent heavy rinsing, conducive for reusable aqueous applications such as biosensors or cellular scaffolding. Zhang *et al.* [41] did the same for cellulose nanofibers, and Chen *et al.* [42] studied the hydrophilicity of thermoplastic polyurethane/collagen blends.

Hong and Kang [43] performed wicking experiments on the differences between conventional nonwovens and electrospun nonwovens. Schoenmaker *et al.* [44] studied the wicking behavior of polyamide (PA) nanofibrous structures with different characteristics.

Hsieh *et al.* [45] focused on understanding how liquids wet, permeate/flow and reside in the porous structure of nanometer size fibrous webs. The aims were to address liquid wetting and flow issues in new nanoporous fibrous materials to meet emerging technical and performance needs in applications, e.g., functional fibers, chemical and biological protective coatings, organic/inorganic catalytic systems, super-absorbent materials, and targeted separation membranes.

Therefore, if the fluid permeability and the wicking property of the electrospun fibers were thoroughly characterized, it would be useful in applying electrospun fibers to specific industrial items, such as filtering materials, electrodes, biomedical membranes and others [43].

The presented method offers the possibility of making coated yarns exhibit the desirable high surface area. The functional requirements of the nanofibers, the structural integrity, mechanical strength of conventional yarns, and the capillary rise of these yarns were also investigated.

## EXPERIMENTAL

### Materials

Nylon 66 multifilament (39.6 denier, 3.96 denier per filament, circular cross-section, and without crimp) was chosen for coating with nylon 66 nanofibers. Commercial nylon 66 chips having a 50,000 (g/mol) molecular weight were prepared by Zanjan Tire Cord. The usable nylon 66 solvent was 98-100% formic acid from Merck Company. Polymer solution with concentrations of 14, 17, 20 wt% was prepared by dissolving and stirring the above mixture with a constant speed in room temperature.

The liquid used for the wicking measurements was single- distillation water with 0.2% non-ionic detergent and 0.5% Methylene Blue (*Figure 1*) for observing the height of the water wicked. This dye is a blue basic dye with low molecular weight of 373.91 g/mol. All wicking measurements were carried out in room conditions.

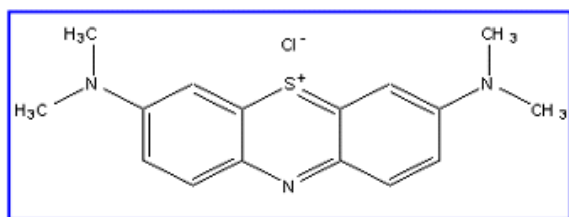


FIGURE 1. Molecular formula of methylene blue.

### Microscopy

The morphology of different nanofibers coating on nylon filament was detected with a Philips scanning electron microscope (XL-30) after gold coating. High magnification SEM images were taken to measure the diameter of nanofibers. The diameters of 100 nanofibers were measured by means of Measurement Software and compared with the image scale. Finally, the average of the results was obtained (*Figure 2*). *Table I* shows the statistical results of fiber diameter measurements.

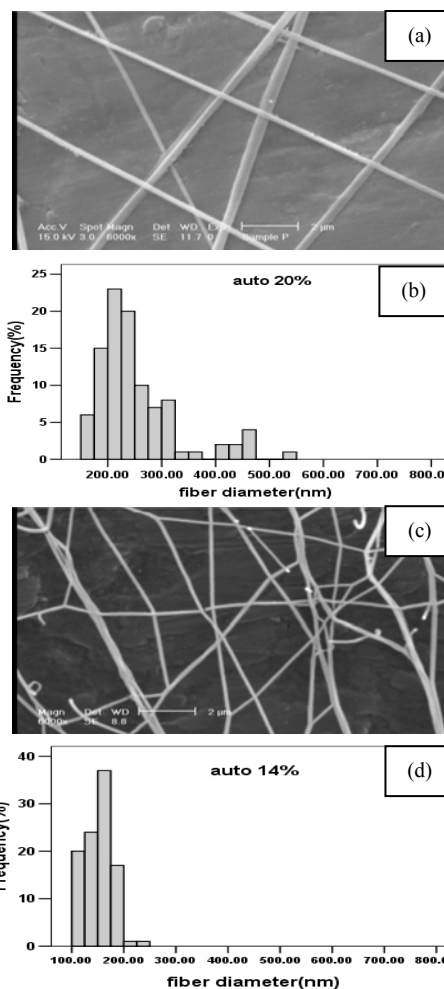


FIGURE 2. Typical SEM images of nylon66 nanofiber in spinning triangle and diameter distribution in different concentrations (a,b) 20% , (c,d) 14%.

TABLE I. Statistical results of fiber diameter.

Concentration	Average Nanofiber Diameter	$\sigma$	CV%
14%	151	25.3	16.75
17%	175	24.5	14
20%	252	75.8	30

### Electrospinning Setup

The nanofiber coating set up shown in *Figure 3* is an in-house-developed technology. Two nozzles were positioned opposite each other with different charges. Electrospun nanofibers were produced with the same charge as their nozzles. A neutral circular plate with a small hole at the center was positioned in the middle of the electric field in order to act as a twister.

The electrostatic inductions happened in the neutral plate, which was placed near the two charged nozzles. It means that the negative charged nozzle attracted positive charges on the side of the neutral plate facing it, while the positive charged nozzle attracted negative charges on the other side of the neutral plate.

The charged jets of polymer solution moved toward the part of circular plate with opposite charge and nanofibers were gathered on this plate.

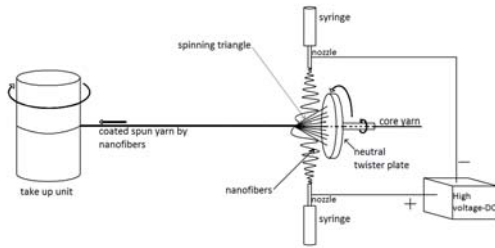


FIGURE 3. Schematic illustration of electrospinning setup for producing nanofiber-coated yarn.

A yarn as a core one was introduced to spinning zone right through the plate center. Electrospun nanofibers come into contact with the yarn's surface and as they are pulled towards the plate, form a spinning triangle. *Figure 3* shows the spinning triangle placed on the twister. Rotating the twister will transfer twisting movement to the nanofibers and lead them to wrap around the yarn. The electrospinning coating is continued by withdrawing the yarn from a bobbin and directing it towards the coating zone. A take-up unit was used to gather the coated yarn.

To produce coated yarns with nanofiber, the optimized parameters of the process were used. The distance between the two nozzles was 13cm and that between neutral circular plate and centre of electric field was 3 cm. Plate diameter was 7cm. The diameter and length of the two nozzles were 0.7 mm and 3.5 cm respectively. The distance between the two nozzles centers and take-up unit was 25 cm. 13 kV voltage was applied. Take-up speed and twist per meter for coating yarns with nanofiber were 6.55 m/hr and 192 TPM, respectively.

Four samples: nylon filament, nylon filament coated with nylon 66 nanofiber in three optimized concentrations of 14%, 17% and 20% without beads and breakage were used in a constant feeding rate (0.21 ml/h).

The typical SEM images of nanofiber-coated filaments are shown in *Figure 4*. The mean linear density of nanofibers coated yarns was about 41.3 den. The twist was the same for all samples.

### Capillary Tests

In this work, a method consisting of observing and measuring the capillary flow of a colored liquid was used. The yarn is placed perpendicular to a liquid bath [3, 5].

*Figure 5* shows schematic representation of the apparatus designed for capillary height measurement. The yarn is fixed to a holder that comes into contact with the liquid in a beaker. A Sony digital handy cam (DCR-PC115E) was used to make video films of colored liquid rise in coated filament with nanofibers for capillary flow. Fast-Forward, a digital graphic adapter, transmitted the video signal from camera to the computer. The camera had a resolution of 720×576 pixels and magnification of 1X - 120X. Frame rate of this camera was 24 frames per second (FPS). In order to characterize any liquid flow (the average of liquid height) of the coated yarn with nanofibers, Windows movie maker was applied to make screen capture. Measurement software was used to gain a set of points at given times from the capillary rise of the colored liquid into the coated yarns ( $t, h$ ). Before doing capillary tests, coated yarns with nanofibers were kept in standard condition:  $(20 \pm 2)^\circ\text{C}$  and 65% relative humidity. For capillary height measurement, each sample was cut into 18 cm length pieces and yarns were kept at constant tension (about 0.1 g/den) on a holder (*Figure 5*). Video films were repeated 10 times for each kind of yarn capillary rise.

### THEORY OF WICKING

In fibrous structures, the capillary flow follows the Eq. (1), which provides the variation of the liquid height  $h$  as a function of time  $t$  in a capillary of radius  $r$  by Poiseuille's law [3]:

$$\frac{dh}{dt} = \frac{R_D^2}{8\eta h} \left[ \frac{2\gamma \cos \theta}{R_S} - \rho gh \right] = \frac{R_D^2 \Delta P}{8\eta h} \quad (1)$$

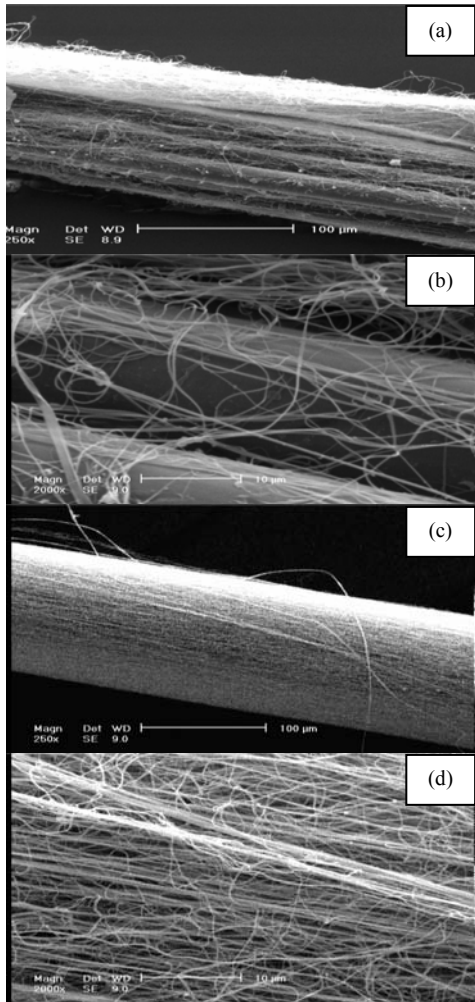


FIGURE 4. SEM images of nylon 66 nanofiber-coated yarn with different concentrations of coating polymer solution (a,b) 20% (c,d) 14%.

where  $h$  is the height of the liquid at time  $t$ ;  $\eta$ ,  $\rho$ , and  $\gamma$  are the viscosity, density, and surface tension of the liquid, respectively;  $\theta$  is the advancing contact angle of the liquid on the surface;  $g$  is the acceleration due to gravity;  $R_D$  is the mean hydrodynamic radius of the pores; and  $R_S$  is the mean static radius of the pores, which is equal to the geometrical radius of the pores. The hydrodynamic radius also depends on the tortuosity of the pores.

At equilibrium ( $\Delta P = 0$ ), the maximum height  $h_{eq}$ , reached by the liquid front, is given by:

$$h_{eq} = \frac{2\gamma \cos \theta_{eq}}{\rho g R_s} \quad (2)$$

where  $\theta_{eq}$  is the equilibrium, static, contact angle, which is generally smaller than the dynamic one.

The pressure difference ( $\Delta P$ ) involves the capillary pressure and the pressure due to gravity. In the early stages of the wicking phenomenon, the hydrostatic pressure can be neglected, and the Washburn equation can be yielded by the integration of Eq. (1):

$$h^2 = \frac{r \gamma \cos \theta}{2\eta} t \quad (3)$$

Where  $r = r_D^2/r_S$  is an equivalent radius of the capillary porous structure. Therefore, the values of  $h^2$  might vary linearly with time as follows:

$$h^2 = At \quad (4)$$

Where

$$A = \frac{r \gamma \cos \theta}{2\eta} \quad (5)$$

Here, the slope is the capillary rate coefficient [3, 5 and 46].

Some researchers have considered capillary rise phenomenon at very last limits as follows:

$$h(t) = h_{eq} \left[ 1 - \exp\left(-\frac{\rho g r^2}{8\eta h_{eq}} t\right) \right] \text{ when } t \rightarrow \infty \quad (6)$$

Some others have studied the behavior of capillary rise at initial times, i.e., when,  $t \rightarrow 0$  or where,  $h \ll h_{eq}$ , as we proposed in this work.

To apply Washburn's equation to wicking studies, numerous researchers established that the wicking height of liquid in a fiber or yarn is proportional to the square root of the time, assuming that gravity is negligible as long as the wicking height is small [3,5,46-48].

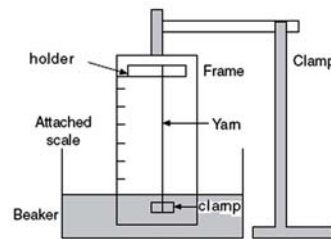


FIGURE 5. Schematic of experimental set up for capillary rise measurements.

## RESULTS AND DISCUSSION

A set of points (t, h) were gained at given times from the capillary rise of the colored liquid to analyze the kinetics of capillary flow in coated yarns with nanofiber. As shown in *Figure 6*, nylon filament without any coating has the least wicking height. Nanofiber-coated filament with 14% polymer concentration has the most wicking height.

As a result, yarn coating with nanofiber increases the equilibrium wicking height. Because of the large specific surface area, nanofibers coated on filaments absorb fluids very efficiently. Also, nanofibers with higher diameter, which have bigger pores, cause a decrease in the equilibrium wicking height. This is consistent with Eq. (2).

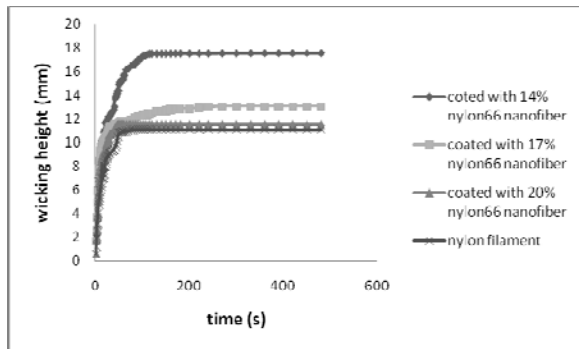


FIGURE 6. Wicking height of nylon filament and nanofiber-coated filaments.

In experimental values, the curve obtained from the height squared as a function of time at initial times (0–30 s) is linear. The Lucas-Washburn equation is valid for the kinetics of capillary flow in yarns if linear regression coefficient is  $R^2 > 0.99$  [5].

In this work, as shown by *Figure 7*, when time is smaller than 30 s, linear regression coefficient  $R^2$  is higher than 0.99. So the kinetics of capillary flow of colored liquid in coated yarns with nanofiber follows the Lucas-Washburn equation (Eq. (4)). The slope of linear fit of experimental data determined the rate of the liquid capillary rise in initial times. *Figure 7* shows the typical variation trend of capillary rise rate by changing yarn samples.

According to our previous work on wicking phenomenon in nanofiber yarns [49], the Lucas-Washburn law is always followed by the experimental points, which give straight lines with different slopes by repeating the capillary process on different pieces of a specific yarn.

It could be concluded that the capillary rise rate coefficient is not unique but varies along the yarn and the yarn heterogeneity causes the variation of this coefficient. As the yarn structure is heterogeneous, during capillary wicking, at each time, the mean level of the liquid in the required number of samples was measured.

The number of tests required to give the mean to an accuracy of 2.5 percent at 95 percent confidence level was 10 samples according to the following equation

$$N = \left( \frac{1.96 \times 100 \times S.D.}{P \times \text{mean}} \right)^2 \quad (7)$$

where *S.D.* and *mean* are standard deviation and average of the capillary rise rate coefficients, respectively. *N* is the number of tests and *P* is the percentage accuracy [50].

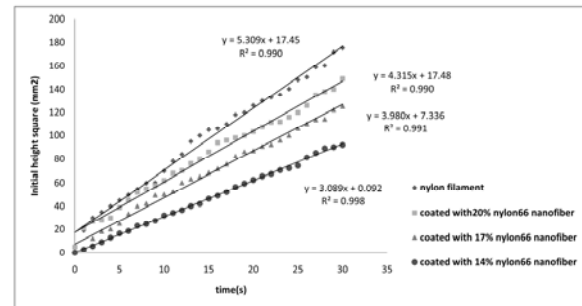


FIGURE 7. Square height of the capillary rise on nylon filament and nanofiber-coated filaments.

This shows that nylon filament had the highest capillary rate  $5.3 \text{ mm}^2/\text{s}$  and the capillary rate of nylon filament coated with 14%, 17% and 20% nylon66 nanofiber are about 3, 4 and  $4.3 \text{ mm}^2/\text{s}$ , respectively.

As shown in *Figure 7*, capillary rise rates have a contradictory order in comparison with equilibrium wicking height in *Figure 6*. The increase in the concentration of polymer solution from 14% to 20% increases capillary rise rate. Because the mean nanofiber diameters of 14%, 17% and 20% in polymer solution were  $151 \pm 25.3$ ,  $175 \pm 24.5$ ,  $252 \pm 75.8 \text{ nm}$ , respectively, this leads to smaller pore size for lower concentration when compared with the higher concentration.

According to Eq. (3), bigger pores in the higher concentration of nanofibers increase capillary rise rate because wicking permeability is increased.

## CONCLUSION

This work developed a new method that allows yarn coating with nanofibers. This method could be applied for any yarns with different nanofiber coatings. Yarn coating with nanofiber could create special properties. In this work, capillary rise of colored liquid along the coated yarns by optical system was investigated. In fibrous structures, the capillary flow follows the Lucas-Washburn's equation at the early steps of the process, given the fact that the hydrostatic pressure can be almost imperceptible. In experimental values, the curve obtained from the height square as a function of time at initial times (0–30s) is linear. The Lucas-Washburn Equation is valid for the kinetics of capillary flow in yarns if linear regression coefficient is  $R^2 > 0.99$  [5]. The kinetics of capillary flow of colored liquid in coated yarns with nanofiber follows the Lucas-Washburn equation. The slope of linear fit of experimental data determines the rate of the liquid capillary rise. Yarn coating with nanofiber increased the equilibrium wicking height. The increase in polymer concentration of nanofiber coating in a process with a constant feeding rate increases capillary rise rate.

## REFERENCES

- [1] Kamath, Y.K.; Hornby, S.B.; Weigmann, H.D.; Wilde, M.F. "Wicking of spin finishes and related liquids into continuous filament yarns", *Textile Res. J.*, 1994, 64(1), 33-40.
- [2] Hsieh, Y.L.; Yu, B. "Liquid wetting, transport, and retention properties of fibrous assemblies, Part I: Water wetting properties of woven fabrics and their constituent single fibers", *Text. Res. J.*, 1992, 62(11), 677–685.
- [3] Kissa, E. "Wetting and wicking", *Textile Res. J.*, 1996, 66(10), 660-668.
- [4] Kornev, K.G.; Neimark, A.V. "Spontaneous penetration of liquids into capillaries and porous membranes revisited", *J. Colloid. Interf. Sci.*, 2001, 235(1), 101-113.
- [5] Perwuelz, A.; Mondon, P.; Caze, C. "Experimental study of capillary flow in yarns", *Textile Res. J.*, 2000, 70(4), 333-339.
- [6] Patnaik, A.; Rengasamy, R. S.; Kothari, V. K.; Ghosh, A. "Wetting and wicking in fibrous materials", *Textile Progress*, 2006, 38(1), 1-105.
- [7] Hollies, N.R.S.; Kaessinger, M.M.; Watson, B.S.; Bogaty, H. "Water transport mechanisms in textile materials. Part II: Capillary-type penetration in yarns and fabrics", *Textile Res. J.*, 1957, 27, 8-13.
- [8] Kamath, Y.K.; Hornby, S.B.; Weigmann, H.D.; Wilde, M.F. "Wicking of spin finishes and related liquids into continuous filament yarns", *Textile Res. J.*, 1994, 64(1), 33-40.
- [9] Sengupta, A.K.; Murthy, H.V.S. "Wicking in ring-spun vis-a-vis rotor-spun yarns", *Indian J. Fiber Text. Res.*, 1985, 10(4), 155–157.
- [10] Chattopadhyay, R.; Chauhan, A. "Wicking behavior of compact and ring spun yarns and fabrics", In One Day Seminar on Comfort in Textiles, Dept. of Textile Technology, I I T Delhi, New Delhi, India, 2004, October 16, p. 20.
- [11] Sengupta, A.K.; Kothari, V.K.; Rengasamy, R.S. "Wicking behavior of air-jet textured yarns", *Indian J. Fiber Text. Res.*, 1991, 16(2), 123–127.
- [12] Ansari, N.; Haghighat Kish, M. "The wicking of water in yarns as measured by an electrical resistance technique", *J. Text. Inst.*, 2000, Part 1, 91(3), 410–419.
- [13] Minor, F.W.; Schwartz, A.M.; Wulkow, E.A.; Buckles, L.C. "The migration of liquids in textile assemblies. Part II: The wicking of liquids in yarns", *Text. Res. J.*, 1959, 29(12), 931–939.
- [14] Adamson, A.W. The Solid–Liquid Interface–Contact Angle, In Physical Chemistry of Surfaces, John Wiley: New York, 1990, p. 379.
- [15] Zhou, F.L.; Gong, R.H.; Porat, I. "Nanocoating on filaments by electrospinning", *Surf. Coat. Technol.*, 2009, 204(5), 621-628.
- [16] Arridge, R.G.C.; Heywood, D. "The freeze-coating of filaments", *Br. J. Appl. Phys.*, 1967, 18, 447-457.
- [17] Hosseini, S.H.; Pairovi, A. "Preparation of conducting fibres from cellulose and silk by polypyrrole coating", *Iran Polym. J.*, 2005, 14(11), 934-940.
- [18] Xue, P.; Tao, X.M. "Morphological and Electromechanical Studies of Fibers Coated with Electrically Conductive Polymer", *J. Appl. Polym. Sci.*, 2005, 98(4), 1844-1854.
- [19] Najjar, S.S.; Kaynak, A.; Foitzik, R.C. "Conductive wool yarns by continuous vapour phase polymerization of pyrrole", *Synth. Met.*, 2007, 157, 1-4.
- [20] Kuraishi, K.; Iwata, H.; Nakano, S.; Kubota, S.; Toonami, H.; Toda, M.; Toma, N.; Matsushima, S.; Hamada, K.; Ogawa, S.; Taki, W. "Development of nanofiber-covered stents using electrospinning: in vitro and acute phase in vivo experiments", *J. Biomed. Mater. Res. B. Appl. Biomater.*, 2009, 88(1), 230-239.

- [21] Abidian, M.R.; Martin, D.C. "Multifunctional Nanobiomaterials for Neural Interfaces", *Advance Function Material*, 2009, 19(4), 573-585.
- [22] Jalili, N.; Goswami, B.C.; Dawson, D. et al, "Distributed Sensors and Actuators via Electronic-Textiles", *National Textile Center Annual Report* (NTC Project: M04-CL05), September 2007.
- [23] Underhill R.S. "The Multifunctional Materials Needs of the Future Dismounted Soldier", *Can. Army J.*, 2009, 12, 61-74.
- [24] Zhou, F.L.; Gong, R.H.; Porat, I. "Nano-coated hybrid yarns using electrospinning", *Surf. & Coat. Technol.*, 2010, 204, 3459-3463.
- [25] Jiang, K.; Li, Q.; Fan, S. "Nanotechnology: Spinning continuous carbon nanotube yarns", *Nat.*, 2002, 419, 801-801.
- [26] Dalton, A.B.; Collins, S.; Munoz, E.; Razal, J.M.; Ebron, V.H.; Ferraris, J.P.; Coleman, J.N.; Kim, B.G.; Baughman, R.H. "Super-Tough Carbon-Nanotube Fibres", *Nat.*, 2003, 423, 703-703.
- [27] Thorvaldsson, A.; Stenhamre, H.; Gatenholm, P.; Walkenstrom, P. "Electrospinning of highly porous scaffolds for cartilage regeneration", *Biomacromol*, 2008, 9, 1044-1049.
- [28] Doshi, J.; Reneker, D.H. "Electrospinning process and applications of electrospun fibers", *J. Electrostatics*, 1995, 35(2-3), 151-60.
- [29] Reneker, D.H.; Yarin, A.L.; Fong, H.; Koombhongse, S. "Bending instability of electrically charged liquid jets of polymer solutions in electrospinning", *J. Appl. Phys.*, 2000, 87(9), 4531-4547.
- [30] De Vrieze, S.; Westbroek, P.; Van Camp, T.; Van Langenhove, L. "Electrospinning of chitosan nanofibrous structures: feasibility study", *J. Mater. Sci.*, 2007, 42(19), 8029-8034.
- [31] Huang, Z.M.; Zhang, Y.Z.; Kotaki, M.; Ramakrishna, S. A. "Review on polymer nanofibers by electro-spinning applications in nanocomposites", *Compos. Sci. Technol.*, 2003, 63, 2223-2253.
- [32] Fang, J.; Niu, H.T.; Lin, T.; Wang, X.G. "Applications of electrospun nanofibers", *Chin. Sci. Bull.*, 2008, 53(15), 2265-2286.
- [33] Liang, D.; Hsiao, B.S.; Chu, B. "Functional electrospun nanofibrous scaffolds for biomedical applications", *Adv. Drug Delivery Rev.*, 2007, 59(14), 1392-1412.
- [34] Yoo, H.S.; Kim, T.G.; Park, T.G. "Surface-functionalized electrospun nanofibers for tissue engineering and drug delivery", *Adv. Drug Delivery Rev.*, 2009, 61(12), 1033-1042.
- [35] Agarwal, S.; Wendorff, J.H.; Greiner, A. "Use of electrospinning technique for biomedical applications", *Polymer*, 2008, 49(26), 5603-5621.
- [36] Smidt, D.; Reneker, D.H., 2001, PCT/U.S. Pat. 00/27737.
- [37] Huang, C.; Chen, S.; Lai, C.; Reneker, D.H.; Qiu, H.; Ye, Y.; Hou, H. "Electrospun polymer nanofibres with small diameters", *Nanotech.*, 2006, 17, 1558-1563.
- [38] Gopal, R.; Kaur, S.; Ma, Z.; Chan, C.; Ramakrishna, S.; Matsuura, T. "Electrospun nanofibrous filtration membrane", *J. Membr. Sci.*, 2007, 281, 581-586.
- [39] Norris, I.D. et al. "Electrostatic Fabrication of Ultrafine Conducting Fibers: Polyaniline/Polyethylene Oxide Blends" *Synth. Met.*, 2000, 114, 109-114.
- [40] Jabal, J.M.F.; McGarry, L.; Sobczyk, A.; Aston, D.E. "Wettability of Electrospun Poly(vinylpyrrolidone)-Titania Fiber Mats on Glass and ITO Substrates in Aqueous Media" *ACS Appl. Mater. Interfaces*, 2009, 1(10), 2325-2331.
- [41] Zhang, H.; Nie, H.; Li, S.; Branford White, C. J.; Zhu, L. "Crosslinking of electrospun polyacrylonitrile/hydroxyethyl cellulose composite nanofibers", *Mater. Lett.*, 2009, 63(13-14), 1199-1204.
- [42] Chen, R.; Qiu, L.; Ke, Q.; He, C.; Mo, X. "Electrospinning Thermoplastic Polyurethane-Contained Collagen Nanofibers for Tissue-Engineering Applications", *J. Biomater. Sci. Polym. Ed.*, 2009, 20(11), 1513-1536.
- [43] Hong, K.H.; Kang, T.J. "Hydraulic permeabilities of PET and nylon 6 electrospun fiber webs", *J. Appl. Polym. Sci.*, 2006, 100(1), 167-177.
- [44] De Schoenmaker, B.; Der Schueren, L.V.; De Vrieze, S.; Westbroek, P.; De Clerck, K. "Wicking properties of various polyamide nanofibrous structures with an optimized method", *J. Appl. Polym. Sci.*, 2011, 120(1), 305-310.
- [45] Hsieh, Y.L.; Pan, N.; Neimark, A.V. "Liquid Wetting and Flow in Nano-Fibrous Systems: Multi-scale and Heterogeneous", National Textile Center Briefs, NTC Project: M04-CD01, 2007.

- [46] Doakhan, S.; Hosseini Ravandi, S.A.; Gharehaghaji, A.; Mortazavi, S.M. "Capillary Rise in Core-spun Yarn", *Iranian Polymer Journal*, 2007, 16(6), 397-408.
- [47] Zhong, W.; Ding, X.; Tang, Z.L. "Modeling and analyzing liquid wetting in fibrous assemblies", *Textile Res. J.*, 2001, 71, 762-766.
- [48] Laughlin, R.D.; Davies, J.E. "Some Aspects of Capillary Absorption in Fibrous Textile Wicking", *Textile Res. J.*, 1961, 31, 904-910.]
- [49] Musavi Jad, M.S.; Hosseini Ravandi, S.A.; Tavanai, H.; Hashemi Sanatgar, R. "Wicking Phenomenon in Polyacrylonitrile Nanofiber Yarn", *Fibers and Polymers*, 2011, 12(6), 801-807.
- [50] Booth, J.E. In Principles of Textile Testing. Butterworth & Co: London, 1968.

#### **AUTHORS' ADDRESSES**

**Seyed Abdolkarim Hosseini Ravandi, PhD**

**Razieh Hashemi Sanatgar, MD**

**Farzad Dabirian, PhD**

Isfahan University of Technology

Daneshgah St.

Isfahan, Isfahan 8415683111

IRAN